

## Synthesis and Third-order Optical Nonlinearity of Mesoporous Au/ZrO<sub>2</sub> Thin Films

LU Qiang<sup>1</sup>, CUI Fang-Ming<sup>2</sup>, WEI Chen-Yang<sup>3</sup>, HUA Zi-Le<sup>3</sup>, DONG Chang-Qing<sup>1</sup>

(1. North China Electric Power University, Beijing 102206, China; 2. Chinese Academy of Space Technology, Beijing 100081, China; 3. Shanghai Institute of Ceramics, Chinese Academy of Sciences, Shanghai 200050, China)

**Abstract:** Highly dispersed gold nanoparticles incorporated mesoporous zirconia thin films were synthesized through an easy deposition-precipitation method using urea as precipitator. The resultant composite thin films presented an enhanced off-resonant third-order optical nonlinear susceptibility of  $10^{-10}$  esu measured by Z-scan technique at 1064 nm. The enhanced optical nonlinearity of the composite thin films was attributed to the high dispersion of the gold nanoparticles and the high linear refractive index of the zirconia matrix.

**Key words:** Au nanoparticles; mesoporous; ZrO<sub>2</sub> thin films; third-order optical nonlinearity

The noble metal nanoparticles (NPs) incorporated dielectric matrix solid thin films with outstanding third-order optical nonlinearities have been widely investigated due to their potential application in the next generation of optical communication and logic processing devices<sup>[1-9]</sup>. Among them, gold NPs incorporated mesoporous thin films have shown reasonably high third-order optical nonlinear susceptibilities ( $\chi^{(3)}$ ) from  $10^{-11}$  to  $10^{-8}$  esu due to the high dispersion of the incorporated gold NPs resulted by the mesoporous channel confinement<sup>[7]</sup>, compared with the composite thin films prepared by physical deposition method<sup>[5-6]</sup>. For example, the gold NPs incorporated mesoporous silica thin films have shown the  $\chi^{(3)}$  of  $5.62 \times 10^{-11}$  esu and an ultrafast optical response of 190 fs measured by optical Kerr effect using an incident laser with 800 nm wavelength<sup>[7]</sup>. And the gold NPs incorporated mesoporous titania thin films have been demonstrated more higher off-resonant  $\chi^{(3)}$  of  $10^{-8}$  esu measured by Z-scan technique at 1064 nm<sup>[9]</sup>.

Recently, ordered mesoporous zirconia thin films (MZTFs) have been successfully synthesized by Sanchez group through the evaporation induced self-assembly method using nonionic surfactants as structure-directing agents<sup>[10-12]</sup>. Compared with other materials, zirconia possesses outstanding thermal and chemical stability and high linear refractive index (2.12), which make it very suitable and promising for optical applications in addition to the conventional industrial applications<sup>[13]</sup>. However, the third-order optical nonlinearities of the mesoporous zirconia-based composite thin films have rarely been investigated. Meanwhile, the more stable and reliable nonlinear optical

thin films with enhanced third-order optical nonlinearities are still highly expected and needed for the future optical applications.

In this paper, highly dispersed gold NPs incorporated MZTFs were successfully synthesized by a facile deposition-precipitation (DP) method using urea as precipitator, which permits a gradual and homogenous addition of hydroxide ions throughout the whole solution and a homogeneous deposition of the metal precursors into the mesoporous channels<sup>[14-17]</sup>. The synthesized gold NPs incorporated MZTFs with 1.2at% gold content showed an enhanced off-resonant  $\chi^{(3)}$  of  $7.08 \times 10^{-10}$  esu measured by Z-scan at 1064 nm, which could be attributed to the high linear refractive index of the zirconia matrix and the high dispersion of the gold NPs.

## 1 Experimental

The MZTFs were prepared by a method combining the procedures reported by Zhao<sup>[18]</sup> and Sanchez<sup>[10-12]</sup>. Firstly, the surfactant F127 were dissolved in anhydrous ethanol (EtOH) solution stirring for 30 min. Secondly, the zirconium (IV) chloride (98% anhydrous) were added into the above surfactant-ethanol solution with stirring, quickly, the solution turned into colorless and transparent. Thirdly, zircon (IV) propoxide (70wt% solution in 1-propanol) were added into the second-step solution with stirring further for 2 h at 26 °C in a closed glass vessel. The composition ratio of the ultimate prepared solution was:  $n(\text{ZrCl}_4):n(\text{Zr}(\text{OC}_3\text{H}_7)_4):n(\text{F127}):n(\text{EtOH})=0.7:0.3:0.01:(30-40)$ . Then, the mesoporous zirconia thin films were prepared

Received date: 2011-08-23; Modified date: 2011-11-15; Published online: 2011-12-10

Foundation item: National Natural Science Foundation of China (51106052); Program for New Century Excellent Talents in University (NCET-10-0374); Fundamental Research Funds for the Central Universities (11QG25)

Biography: LU Qiang (1982-), male, PhD. E-mail: qianglu@mail.ustc.edu.cn

Corresponding author: CUI Fang-Ming, PhD. E-mail: cfm@mail.ustc.edu.cn

by dip-coating in a chamber with relative humidity (RH) of 55% and temperature of 26°C. The clean glass substrate was dipped into the ultimate solution (colorless and transparent) and then withdrew at a rate of 1–5 mm/s. The thin films turned into opaque as soon as the substrate left the zirconia precursor solution. Then, the films turned into transparent again by increasing the RH of the surroundings. Repeat this process twice. The ultimate transparent surfactant-zirconia thin films were aged in the chamber at 26°C and 55% RH for at least 24 h. The surfactant templates were removed by calcination at 350°C for 3 h in air.

The small-angle X-ray diffraction (SAXRD) patterns of the films were conducted in Rigaku Rotaflex diffractometer equipped with a rotating anode and using CuK $\alpha$  radiation. The transmission electron microscope (TEM) images, selective area electron diffraction (ED) pattern and simultaneous energy-dispersive spectroscopy (EDS) spectrum were executed in a JEM-2100F field emission TEM with an accelerating voltage of 200 kV. UV-Vis absorption spectra were measured on Shimadzu UV-3101. The thicknesses and linear refractive indexes of the films were measured to be (233 $\pm$ 10) nm and 1.92 at 1064 nm by SGC-10 film thickness measurement apparatus. The transmittances of the films were measured to be 81.1% by dividing the transmitted laser energy with the incident laser energy. A mode-locked Nd:YAG laser was used in the Z-scan experiment. The laser focused to a beam waist of 35  $\mu$ m at the focus then went through an aperture with an aperture factor of 0.0192. The power of the incident laser was  $1.26 \times 10^6$  ( $\pm$ 5%) W.

## 2 Results and discussion

Figure 1 shows the SAXRD patterns of the air-dried and templates removed MZTF. The two diffraction peaks at  $2\theta = 0.84^\circ$  and  $1.35^\circ$  are indexed as (110) and (200) reflections of the cubic-phased mesoporous structure<sup>[19]</sup> which indicates an ordered mesoporous structure of the

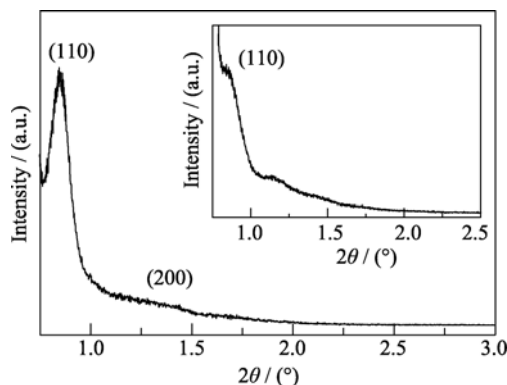


Fig. 1 SAXRD pattern of the air-dried MZTF, and the inset is the template-removed MZTF

prepared zirconia thin films, as seen in Fig. 1. But the periodic ordering of the thin films is partly lost after the surfactant templates are removed by calcination at 350°C for 3 h in the air, as the inset in Fig. 1 shown. From the inset SAXRD pattern, we can see that the (110) reflection is not distinct as that of the air-dried one and moved towards a higher  $2\theta$  region of  $0.85^\circ$ . This may be due to the further contraction and copolymerization of the mesoporous zirconia framework by calcination.

Figure 2 shows the TEM images of the air-dried MZTF and the gold NPs incorporated MZTF. From Fig. 2(a), the ordered arrangement of the cubic-phased mesopores is observed in the air-dried MZTF, as indicated by the two white circles in the image. The circled areas can be indexed as (111) and (100) planes according to the geometry of the cubic-phased mesoporous structure. The result is consistent with the above SAXRD analysis. From Fig. 2(b), we can see the gold NPs (the black dots in the image) highly disperse within the MZTF with an average diame-

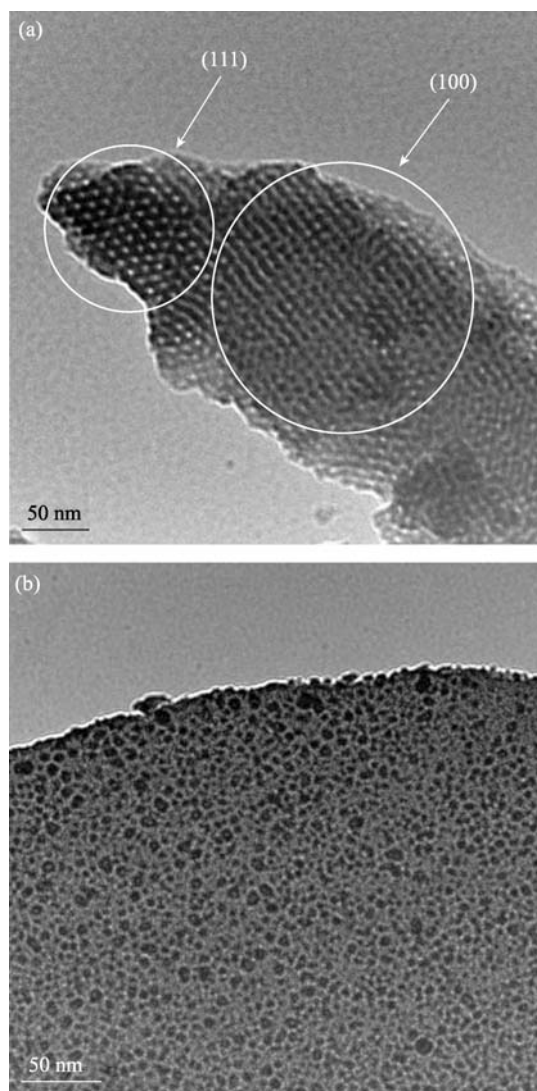


Fig. 2 TEM images of (a) air-dried and (b) gold NPs incorporated MZTF

ter of 6 nm mainly due to the confinement effect of the mesoporous channels<sup>[7, 9]</sup>. The existence of the gold NPs and a semi-quantitative gold content (1.2at%) of the composite thin films can be confirmed and measured by simultaneous EDS spectrum, as seen in Fig. 3, which shows the distinctive signal peaks of the elements Au and Zr.

Figure 4 shows the UV-Vis absorption spectra of the blank MZTF and the gold NPs incorporated MZTF. The blank MZTF did not appear any absorption in the detection region from 350 to 800 nm in the UV-Vis absorption spectra, as seen curve (a) in Fig. 4. While the gold NPs incorporated MZTF presented a distinct absorption peak at 560 nm in the UV-Vis absorption spectra, which was corresponded to the characteristic surface plasmon resonance (SPR) absorption of the gold NPs, as curve (b) in Fig. 4 shown. The SPR absorption peak was apparently red-shifted compared with that (at around 541 nm) of gold NPs incorporated mesoporous silica thin films<sup>[7]</sup> as the dielectric constant of the zirconia matrix is higher than that of the silica matrix<sup>[20]</sup>. The increased background absorption of the gold NPs incorporated MZTF originated from the inter-band transition of valence electrons of the gold NPs from *d* band to the Fermi surface<sup>[21]</sup>.

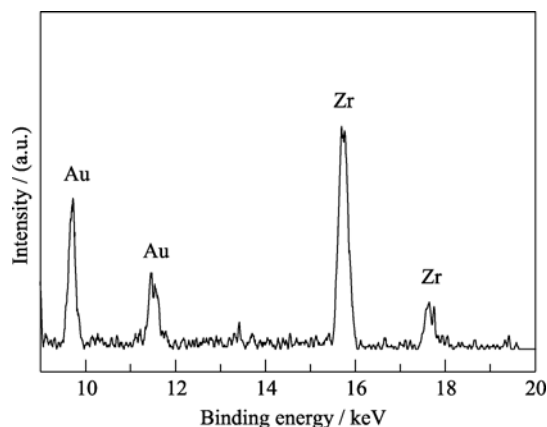


Fig. 3 EDS spectra of the gold NPs incorporated MZTF

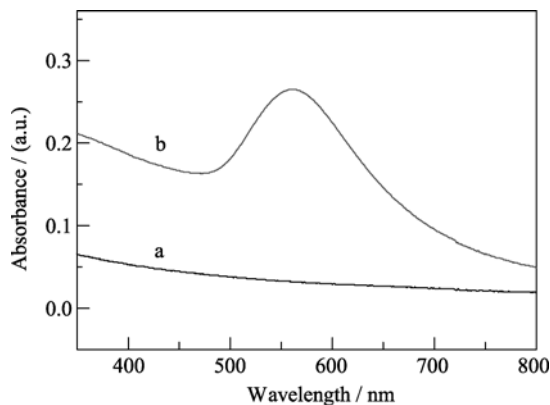


Fig. 4 UV-Vis absorption spectra of (a) blank and (b) gold NPs incorporated MZTF

The third-order optical nonlinearity of the gold NPs incorporated MZTF was measured by Z-scan technique using a 1064 nm incident laser. Both the nonlinear optical (NLO) refraction and absorption of the samples can be measured by Z-scan technique<sup>[22]</sup>.

Figure 5 shows the closed aperture (CA) and open aperture (OA) Z-scan outputs of the gold NPs incorporated MZTF. The CA Z-scan output presented a symmetrical peak followed by a valley in the normalized transmittance trace which indicates a negative NLO refractive index and a self-defocusing NLO process. Neither saturation nor anti-saturation absorption appeared in the OA Z-scan output, indicating that the composite thin films did not have distinctive NLO absorptions, as seen Fig. 5(b). The experimental phenomenon is consistent with that of our previously investigated gold-silica composite thin films mainly due to the off-resonant measurement at 1064 nm<sup>[23]</sup>.

The absolute values of the NLO refractive index ( $n_2$ ) and the  $\chi^{(3)}$  of the gold NPs incorporated MZTF were calculated to be  $3.47 \times 10^{-9}$  and  $7.08 \times 10^{-10}$  esu according the method reported in literature<sup>[23]</sup>. The  $\chi^{(3)}$  of the present material is significantly higher than that ( $\chi^{(3)} \approx 5.62 \times 10^{-11}$  esu) of the highly dispersed gold NPs incorporated mesoporous silica thin films measured by a time-resolved optical Kerr effect at 800 nm<sup>[7]</sup> and comparable with that ( $\chi^{(3)} \approx 8.23 \times 10^{-10}$  esu) of the gold NPs incorporated mesoporous

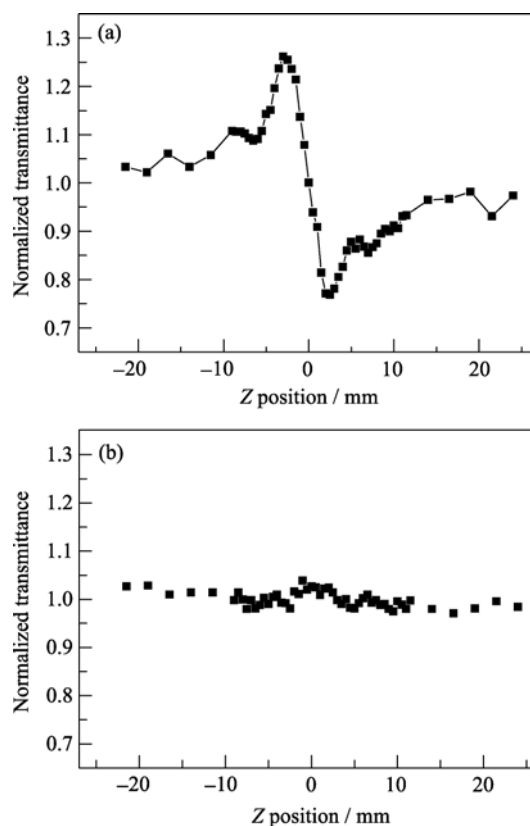


Fig. 5 (a) CA and (b) OA Z-scan outputs of the gold NPs incorporated MZTF

silica thin films with an ultrahigh gold content of 30wt% measured by Z-scan experiment at 1064 nm<sup>[23]</sup>. The relative high  $\chi^{(3)}$  of the gold NPs incorporated MZTF could be attributed to the higher linear refractive index of zirconia matrix (2.1) than that of silica (1.4). So the enhanced off-resonant  $\chi^{(3)}$  of the gold NPs incorporated MZTF may be assigned to the higher linear refractive index of zirconia matrix and the high dispersion of the gold NPs. And the optical nonlinearity of the gold-zirconia composite thin films was believed to originate from the intra-band transition of electrons near the Fermi surface in the incorporated gold NPs<sup>[7]</sup>.

### 3 Conclusions

Highly dispersed gold NPs incorporated mesoporous zirconia thin films were successfully synthesized by an easy deposition-precipitation method. The third-order optical nonlinearities of the composite thin films were measured by Z-scan technique at 1064 nm. The absolute values of optical nonlinear refractive index and third-order optical nonlinear susceptibility of the composite thin films were calculated to be  $3.47 \times 10^{-9}$  and  $7.08 \times 10^{-10}$  esu. The enhanced third-order optical nonlinearity of the material could be attributed to the high linear refractive index of the zirconia matrix and the high dispersion of the gold NPs.

### References:

- [1] Hache F, Ricard D, Flytzanis C, *et al.* Optical nonlinearities of small metal particles: surface-mediated resonance and quantum size effects. *J. Opt. Soc. Am. B*, 1986, **3**(12): 1647–1655.
- [2] Ricard D, Roussignol P, Flytzanis C, *et al.* Surface-mediated enhancement of optical phase conjugation in metal colloids. *Opt. Lett.*, 1985, **10**(10): 511–513.
- [3] Fukumi K, Chayahara A, Kadono K, *et al.* Au<sup>+</sup>-ion-implanted silica glass with non-linear optical property. *Jpn. J. Appl. Phys.*, 1991, **30**: L742–L744.
- [4] Tanahashi I, Manabe Y, Tohda T, *et al.* Optical nonlinearities of Au/SiO<sub>2</sub> composite thin films prepared by a sputtering method. *J. Appl. Phys.*, 1996, **79**(3): 1224–1232.
- [5] Liao H, Xiao R, Fu J, *et al.* Large third-order optical nonlinearity in Au:SiO<sub>2</sub> composite films near the percolation threshold. *Appl. Phys. Lett.*, 1997, **70**(1): 1–3.
- [6] Liao H, Xiao R, Wang H, *et al.* Large third-order optical nonlinearity in Au:TiO<sub>2</sub> composite films measured on a femtosecond time scale. *Appl. Phys. Lett.*, 1998, **72**(15): 1817–1820.
- [7] Gu J, Shi J, You G, *et al.* Incorporation of highly dispersed gold nanoparticles into the pore channels of mesoporous silica thin films and their ultrafast nonlinear optical response. *Adv. Mater.*, 2005, **17**(5): 557–560.
- [8] Xenogiannopoulou E, Iliopoulos K, Couris S, *et al.* Third-order nonlinear optical response of gold island films. *Adv. Funct. Mater.*, 2008, **18**(8): 1281–1289.
- [9] Cui F, Hua Z, He Q, *et al.* Preparation and third-order optical nonlinearity of gold nanoparticles incorporated mesoporous TiO<sub>2</sub> thin films. *J. Opt. Soc. Am. B.*, 2009, **26**(1): 107–112.
- [10] Crepaldi E, Soler-Illia G, Bouchara A, *et al.* Controlled formation of highly ordered cubic and hexagonal mesoporous nanocrystalline yttria–zirconia and ceria–zirconia thin films exhibiting high thermal stability. *Chem. Int. Ed.*, 2003, **42**(3): 347–351.
- [11] Crepaldi E, Soler-Illia G, Grosso D, *et al.* Nanocrystallised titania and zirconia mesoporous thin films exhibiting enhanced thermal stability. *New J. Chem.*, 2003, **27**(1): 9–13.
- [12] Crepaldi E, Soler-Illia G, Grosso D, *et al.* Design and post-functionalisation of ordered mesoporous zirconia thin films. *Chem. Commun.*, 2001, **47**(17): 1582–1583.
- [13] Huang W, Shi J. Synthesis and properties of ZrO<sub>2</sub> films dispersed with Au nanoparticles. *J. Sol-Gel Sci. Tech.*, 2001, **20**(2): 145–151.
- [14] Zanella R, Giorgio S, Henry C R, *et al.* Alternative methods for the preparation of gold nanoparticles supported on TiO<sub>2</sub>. *J. Phys. Chem. B.*, 2002, **106**(31): 7634–7642.
- [15] Yan W, Mahurin S, Chen B, *et al.* Effect of supporting surface layers on catalytic activities of gold nanoparticles in CO oxidation. *J. Phys. Chem. B.*, 2005, **109**(32): 15489–15496.
- [16] Stangland E, Taylor B, Andres R, *et al.* Direct vapor phase propylene epoxidation over deposition-precipitation gold-titania catalysts in the presence of H<sub>2</sub>O<sub>2</sub>: effects of support, neutralizing agent, and pretreatment. *J. Phys. Chem. B.*, 2005, **109**(6): 2321–2330.
- [17] Moreau F, Bond G, Taylor A. Gold on titania catalysts for the oxidation of carbon monoxide: control of pH during preparation with various gold contents. *J. Catal.*, 2005, **231**(1): 105–114.
- [18] Tian B, Liu X, Tu B, *et al.* Self-adjusted synthesis of ordered stable mesoporous minerals by acid-base pairs. *Nat. Mater.*, 2003, **2**: 159–163.
- [19] Zhang Y, Yuwono A H, Li J, *et al.* Highly dispersed gold nanoparticles assembled in mesoporous titania films of cubic configuration. *Micropor. Mesopor. Mater.*, 2008, **110**(2/3):

- 242–249.
- [20] Daniel M, Astruc D. Gold Nanoparticles: assembly, supramolecular chemistry, quantum-size-related properties, and applications toward biology, catalysis, and nanotechnology. *Chem. Rev.*, 2004, **104**(1): 293–346.
- [21] Inouye H, Tanaka K, Tanahashi I, *et al.* Ultra dynamics of non-equilibrium electrons in a gold nanoparticle system. *Phys. Rev. B.*, 1998, **57**(18): 11334–11340.
- [22] Sheik-bahae M, Said A A, Wei T H, *et al.* Sensitive measurement of optical nonlinearities using a single beam. *IEEE J. Quantum Electron.*, 1990, **26**(4): 760–769.
- [23] Cui F, Hua Z, Cui X, *et al.* Au nanoparticles incorporated mesoporous silica thin films with a high Au content: preparation and third-order optical nonlinearity. *Dalton Trans.*, 2009(15): 2679–2682.

## 介孔 Au/ZrO<sub>2</sub> 复合薄膜的制备及其三阶非线性光学性能

陆 强<sup>1</sup>, 崔方明<sup>2</sup>, 魏晨阳<sup>3</sup>, 华子乐<sup>3</sup>, 董长青<sup>1</sup>

(1. 华北电力大学, 北京 102206; 2. 中国空间技术研究院, 北京 100081; 3. 中国科学院 上海硅酸盐研究所, 上海 200050)

**摘 要:** 以尿素为沉淀剂, 通过沉积–沉淀的方法, 制备了高分散的金纳米颗粒负载的介孔氧化锆薄膜; 以 1064 nm 激光为入射光束, 通过 Z 扫描实验测试了复合薄膜的非线性光学折射和吸收, 并计算了复合薄膜的非共振三阶非线性光学极化率( $\sim 10^{-10}$  esu), 金纳米颗粒的高分散性和氧化锆薄膜衬底的高线性折射率使复合薄膜显示了增强的三阶非线性极化率.

**关 键 词:** 金纳米颗粒; 介孔; 氧化锆薄膜; 三阶非线性光学性能

**中图分类号:** TQ174

**文献标识码:** A